Kondo-Transport Spectroscopy of Single Molecule Magnets

C. Romeike,[1] M. R. Wegewijs,[1] W. Hofstetter,[2] and H. Schoeller[1]

[1]*Institut für Theoretische Physik A, RWTH Aachen, 52056 Aachen, Germany*
[2]*Institut für Theoretische Physik, J. W. Goethe-Universität Frankfurt, 60438 Frankfurt am Main, Germany*
(Received 22 May 2006; published 13 November 2006)

We demonstrate that in a single molecule magnet strongly coupled to electrodes the Kondo effect involves all magnetic excitations. This Kondo effect is induced by the quantum tunneling of the magnetic moment. Importantly, the Kondo temperature T_K can be much larger than the magnetic splittings. We find a strong modulation of the Kondo effect as a function of the transverse anisotropy parameter or a longitudinal magnetic field. Both for integer and half-integer spin this can be used for an accurate transport spectroscopy of the magnetic states in low magnetic fields on the order of the easy-axis anisotropy parameter. We set up a relationship between the Kondo effects for successive integer and half-integer spins.

Introduction.—Single molecule magnets (SMMs) allow the study of quantum phenomena on a mesoscopic scale, namely, the quantum tunneling of the magnetic moment. SMMs such as Mn_{12} or Fe_8 have attracted intense experimental and theoretical investigation [1] in recent years. Because of weak intermolecular interaction molecular crystal properties can be assigned to single molecules described by a large spin ($S > 1/2$), and easy-axis and transverse anisotropies. Recently, two groups [2,3] have trapped a *single* molecule magnet (Mn_{12}) in a three terminal transport setup and measured transport through the single molecule. Electron transport fingerprints due to both sequential [2,3] and inelastic cotunneling [3] processes were observed and associated with the molecular magnetic states. Theoretical works [4–6] predicted that fingerprints of magnetic quantum tunneling (QTM) can in principle be identified in transport measurements in the charge (sequential tunneling) as well as in the spin fluctuation (Kondo) regime. Especially the latter regime of strong coupling to the electrodes is of importance since the Kondo effect shows up as a sharp zero-bias anomaly with width given by the Kondo temperature T_K. The Kondo effect has been observed experimentally in many other systems with small spins (e.g., quantum dots [7–11] and single molecules [12,13]). For SMMs with half-integer spin S in zero magnetic field it was shown [5] that the Kondo effect arises from a cooperation of both spin exchange processes with the reservoirs and the intrinsic tunneling of the magnetic moment. The strong coupling fixed point is of pseudo-spin-1/2 type. In this limit the exchange coupling J is weak, such that the resulting Kondo temperature $T_K(J, \Delta) \ll \Delta$, where $\Delta \lesssim 1$ meV is the scale of the anisotropy splittings between the magnetic states. In this case, the Kondo effect involves only the two magnetic ground states of the SMM and does not occur for integer spin.

In this Letter we study the Kondo effect in the experimentally more favorable regime of strong exchange ($J \sim 0.1$ eV) where the Kondo temperature becomes larger than the magnetic splittings $T_K(J, \Delta) \gg \Delta$. We find that *excited* magnetic levels on the SMM, belonging to different topological sectors (with respect to rotations around the z axis), become essentially involved in the Kondo effect. In zero magnetic field and for half-integer spin the Kondo effect can be modulated by changing the transverse anisotropy, resulting in a sequence of Kondo effects associated with different magnetic excited states. A longitudinal magnetic field can induce two important new effects. (1) For both integer and half-integer spin the Kondo effect is suppressed at each anticrossing of magnetic levels belonging to the *same* topological sector. The corresponding sharp magnetic field scale is determined by the transverse magnetic anisotropy. Therefore, the study of the magnetic field dependence allows for an accurate spectroscopy of the magnetic states. This modulation of the Kondo effect allows for an experimental proof of the existence of QTM in a *single* molecule *in a transport junction* and to determine the important microscopic parameters characterizing the SMM in that setup. The *magnetic field induced* Kondo effect for integer spin SMMs allows many molecular magnets like, e.g., Fe_8 to be studied without charging the molecule to obtain a half-integer spin. (2) We find that the Kondo effects for successive integer and half-integer spin S display a close correspondence when shifted in magnetic field energy by the easy-axis anisotropy parameter D.

Model.—We consider a SMM (Fig. 1) in a transport setup where the applied voltages, charging effects, and low temperature suppress single-electron processes [5]. In the presence of a longitudinal magnetic field the Hamiltonian reads $H = H_{SMM} + H_{ex} + H_{res}$:

$$H_{SMM} = -DS_z^2 + \tfrac{1}{2}B_2(S_+^2 + S_-^2) + H_z S_z \qquad (1)$$

$$H_{ex} = J\boldsymbol{S} \cdot \boldsymbol{s} \qquad (2)$$

$$H_{res} = \sum_{k\sigma} \epsilon_{k\sigma} a_{k\sigma}^\dagger a_{k\sigma}, \qquad (3)$$

where S_z is the projection of the SMM's spin on the easy z axis, and $S_\pm = S_x \pm iS_y$. The terms in Eq. (1) describe,
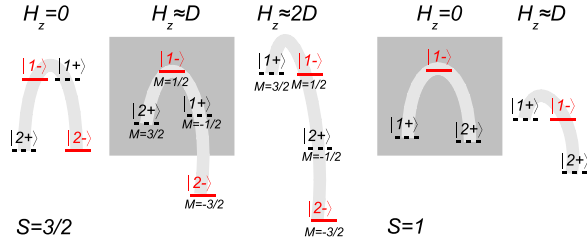
FIG. 1 (color online).   Energy diagram for H_M with $B_2 \ll D$ for various magnetic fields. The two subsets of eigenstates of different magnetic symmetry are indicated by full and dashed bars.

respectively, the easy-axis magnetic anisotropy of the molecule, the transverse anisotropy perturbation, and the coupling to a magnetic field (H_z) along the easy axis. The g factors are absorbed into the magnetic field. For simplicity, we have taken a twofold rotation-symmetry axis, which is dominant in many molecular magnets. The Hilbert space of H_{SMM} is split into two disjoint topological subspaces $\sigma = \pm$ since the twofold rotational symmetry about the z axis is preserved under the longitudinal magnetic field. While for half-integer S these spaces are spanned by an equal number of $n_+ = n_- = S + 1/2$ basis states $\{|S, M\rangle\}_{M=\sigma S, \sigma(S-2),...,-\sigma(S-3),-\sigma(S-1)}$, for integer spin they are spanned by $n_+ = S + 1$ states $\{|S, M\rangle\}_{M=-S,-S+2,...,S-2,S}$ for $\sigma = +$ and by $n_- = S$ states $\{|S, M\rangle\}_{M=-S+1,-S+3,...,S-3,S-1}$ for $\sigma = -$. The eigenstates $|l\sigma\rangle$ of H_{SMM} with energies $E_{l\sigma}$ are labeled by $l = 1, 2, .., n_\sigma$ in order of decreasing energy in each subspace (see Fig. 1). Equation (2) describes the exchange coupling of the molecular spin to the effective reservoir Eq. (3) (bandwidth $2W$ and constant density of states ρ). The electronic states are labeled by $k\sigma$ and denote the even combination of left and right physical electrode states [14,15]. The local electron spin in the reservoir is $s = \sum_{kk'} \sum_{\sigma\sigma'} a_{k\sigma}^\dagger \boldsymbol{\tau}_{\sigma\sigma'} a_{k'\sigma'}/2$, where $\boldsymbol{\tau}$ is the Pauli-matrix vector. The exchange coupling J is induced by virtual electron tunneling processes and is antiferromagnetic due to the strong energy and charge quantization effects. The Kondo spin scattering of conduction electrons off the SMM transfers charge between physical left and right electrodes and can resonantly enhance the linear conductance. The half width at half maximum of the resulting zero-bias differential conductance peak at $T = 0$ is the Kondo temperature T_K.

For a qualitative discussion it is useful to change to the exact representation of Eq. (2) in the eigenbasis of the molecular states $|l\sigma\rangle$:

$$H_{ex} = \sum_{ll'}\left(\sum_{i=x,y} J_{ll'}^i P_{ll'}^i s_i + \sum_\sigma J_{ll'\sigma}^z |l\sigma\rangle\langle l'\sigma|s_z\right). \quad (4)$$

The Hamiltonian Eq. (4) describes the exchange processes involving reservoir electrons and internal magnetic degrees of freedom of the SMM. This projection makes explicit that the QTM parameter B_2 and the external magnetic field

H_z modulate the *effective* couplings through the matrix elements of the molecular spin operator S. The first, transverse, term describes the spin scattering involving a pair of states $|l+\rangle$ and $|l'-\rangle$ in terms of pseudo-spin-1/2 operators $P_{ll'}^x, iP_{ll'}^y = (|l+\rangle\langle l' - | \pm |l'-\rangle\langle l + |)/2$ with effective exchange couplings

$$J_{ll'}^{x/y} = J\langle l + |S_+ \pm S_-|l'-\rangle. \quad (5)$$

In total, there are $n_+ n_-$ such pairs of states from opposite topological sectors. The longitudinal couplings read $J_{ll'\sigma}^z = J\langle l\sigma|S_z|l'\sigma\rangle$. Longitudinal spin operators $P_{ll'}^z = (|l+\rangle\langle l + | - |l'-\rangle\langle l' - |)/2$ can only be introduced in a *unique* way if an approximative projection onto a single pair is made. For instance, one recovers the projection of Ref. [5] onto the ground state pair for zero-field and half-integer S by using time-reversal symmetry and by truncating the excited states. However, such a truncation is not valid in the regime of interest here: the strong exchange coupling J gives rise to a Kondo temperature that can be larger than the magnetic splittings ($T_K \gtrsim 2SD$ for $B_2 \ll D$). The Kondo effect can occur irrespective of whether the pair of states $|l+\rangle$ and $|l'-\rangle$ are ground or excited states of the SMM and whether or not they are exactly degenerate. The Kondo effect therefore involves contributions from multiple topological pairs. This we confirmed explicitly by calculating the projection of the full many-body ground state onto each molecular eigenstate using the numerical renormalization group (NRG). Thus the full expression for H_{ex}, Eq. (4), must be retained for which a *unique* decomposition into a sum of *independent* pairs is not possible. This is due to the fact that a single eigenstate of the SMM $|l\sigma\rangle$ is paired with $n_{-\sigma} > 2$ states $|l' - \sigma\rangle$.

Physical picture.—Variation of either the QTM parameter B_2 or the magnetic field H_z results in anticrossings of magnetic levels. As shown in Fig. 1 the variation of the magnetic field leads to an alternating sequence of degeneracies between pairs of levels which are in different subspaces (crossings) or in the same subspace (anticrossings). Importantly, this occurs in the low magnetic field energy window where the Zeeman splittings are still smaller than T_K ($E_{l\sigma} - E_{l'\sigma'} < T_K$). The effective couplings in Eq. (4) are modulated strongly at each anticrossing leading to a suppression of the Kondo effect on a scale $\sim B_2$, as we now explain. At an anticrossing states $|l\sigma\rangle$ and $|l'\sigma\rangle$ from the *same* topological sector are close in energy and strongly hybridize due to the transverse anisotropy. Following two levels *adiabatically* during an anticrossing they interchange their role and one basis state picks up a relative phase π. For example, in Fig. 1 the level $|1+\rangle$ is moving upwards and the level $|2+\rangle$ downwards in energy after the anticrossing. For *each* topological pair involving one of the anticrossing levels this leads to a sign change of one of the transverse couplings, as can be seen easily from Eq. (5). The latter therefore vanish at the anticrossing and the Kondo effect is expected to be suppressed. This happens on a magnetic field scale proportional to the tunnel split-

ting, i.e., will occur as a sharp feature in the linear con-
ductance as function of a longitudinal magnetic field. In a
similar way, in zero field the variation of the QTM parame-
ter B_2 itself leads to a series of anticrossings, which for a
half-integer spin preserves the twofold Kramers degener-
acy of all levels. This happens due to the nonuniform level
spacing and the coupling of states occurs in different orders
of perturbation theory in B_2 (higher-lying levels hybridize
more strongly for weak B_2).

Method.—We use Wilsons's NRG [16,17] to treat non-
perturbatively the full model $H = H_{SMM} + H_{ex} + H_{res}$. As
NRG input parameters we use number of states $N = 1000$,
discretization $\Lambda = 2$, and $D = 10^{-4}$ W. We analyzed the
NRG level flow as function of iteration number N_{iter} in or-
der to determine the low-temperature fixed point for $H_z =
0$. The Kondo temperature is defined as the energy scale
where the crossover to strong coupling takes place. We also
calculated the spectral function within the T-matrix ap-
proach [18]: $A_\sigma(\omega) = -\frac{1}{\pi} \text{Im} T_\sigma(\omega + i\delta)$, where the T ma-
trix is $T_\sigma(\omega) = \langle\langle O_\sigma; O_\sigma^\dagger \rangle\rangle$ with $O_\sigma = \frac{J}{2}(c_{0,-\sigma}S^{-\sigma} +
\sigma c_{0,\sigma}S_z)$ and $c_{0,\sigma} = \sum_k c_{k,\sigma}$ is the electron operator on
the first site of the Wilson chain. The low-temperature
conductance $G = -(e^2/2)\sum_\sigma \int d\omega A_\sigma(\omega)df(\omega)/d\omega$ is
proportional to the spectral function, where $f(\omega) =
1/(e^{\omega/T} + 1)$. The effects considered here are difficult to
capture in a poor-man's scaling approach due to the strong
coupling and the many excited states involved. However,
another useful guide to the full NRG results in this regime
is the spin-binding energy ΔE, obtained by diagonalizing
exactly the molecular Hamiltonian Eq. (1) coupled by
exchange to a *single* conduction electron spin. This is
similar to the first step of a NRG calculation and will be
denoted as the zero-bandwidth model. The ground- to
excited-state gap ΔE thus obtained follows the modulation
of T_K by B_2 and H_z accurately, although the scales of ΔE
and T_K strongly differ. Apparently, for a sizable range of
the relevant exchange strengths $J < W$ the zero-bandwidth
estimate ΔE is renormalized *uniformly* by the coupling to
the remaining conduction band electrons. This estimate
breaks down when the modulation involves a suppression
of T_K far below the scale of the magnetic splittings: then
the renormalization becomes nonuniform and the variation
may deviate from the NRG.

Kondo effect due to excited states tuned by QTM.—We
first consider the case of zero magnetic field. For integer
spin this corresponds to an anticrossing: the eigenstates are
paired to nearly degenerate states from the same subspace
which are splitted by the transverse anisotropy. Conse-
quently, as discussed above the Kondo effect is suppressed,
resulting even in a *dip* in the spectral function, see below.
In contrast, for half-integer spin many topological pairs are
degenerate (crossing) due to time-reversal symmetry, see
Fig. 1. The NRG converges to the spin-1/2 strong coupling
fixed point, indicating a complete screening of the mag-
netic degrees of freedom. As shown in Fig. 2(a) the Kondo
temperature shows an oscillatory dependence on B_2/D.

The number of oscillations for $0 \leq B_2 \leq D$ is $S - 1/2$.
When decreasing the exchange coupling J the smallest
peaks disappear first, leaving only the monotonic increase
of T_K up to the broad maximum centered at $B_2 \sim D$ in the
limit where the magnetic excitations can be neglected [5].
The spin-binding energy ΔE captures this dependence on
B_2/D, as shown in Fig. 2(b). Interestingly, we find that the
nature of the ground state of the zero-bandwidth model
changes with each oscillation which can in turn be related
to an anticrossing of magnetic states on the SMM. For
instance, for weak $B_2 \ll D$ near the lowest peak in
Fig. 2(b) the highest *excited* Kramers doublets are strongly
mixed into the zero-bandwidth model ground state. In
contrast, for $B_2 \sim D$ near the highest peak in Fig. 2(b)
the ground doublet dominates in the ground state. This
demonstrates that the observed strong coupling Kondo
fixed point in the NRG indeed originates from a screening
of magnetic degrees of freedom involving excited mag-
netic states of the SMM. Which of these excited states are
important depends on B_2/D.

Kondo-spectroscopy of SMMs.—We now focus on the
most relevant case of fixed weak QTM ($B_2 \ll D$) and vary
the longitudinal magnetic field H_z. For many magnetic
field values the spectral density shown in Figs. 3(a)–3(d)
displays a zero-bias Kondo resonance. The corresponding
many-body ground state found in the NRG at the strong
coupling fixed point is nondegenerate. This peak is
strongly modulated at avoided crossings of states from
the same subspace at $H_z/D \approx 2k$ $(2k + 1)$, $k = 1, 2, \ldots$
for integer (half-integer) spin. As discussed above, this is
related to the strong suppression of effective exchange
couplings on the magnetic field scale B_2 near an anticross-
ing. In contrast, the spectral function varies smoothly at
level crossings located at $H_z/D \approx 2k + 1$ $(2k)$ for integer
(half-integer) spin. In this way the two scales D and B_2 can
be identified in the magnetic field dependence of the linear
conductance. For integer spin $S = 1$ the spectral function
in Fig. 3(a) shows a dip for $H_z = 0$ (anticrossing of $|1+\rangle$
and $|2+\rangle$). At fields $H_z \sim B_2$ a Kondo peak is *induced*
which reaches maximal height at $H_z = D$ (crossing of
$|1+\rangle$ and $|1-\rangle$). This Kondo peak is subsequently sup-
pressed and split due to the Zeeman level shifts, see Fig. 1.
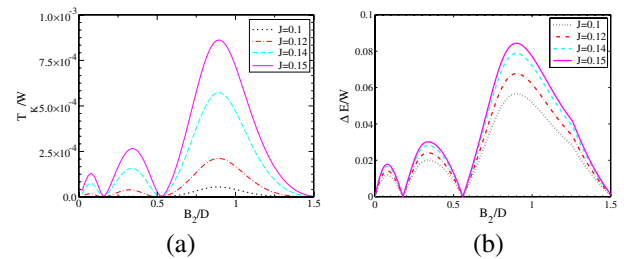For half-integer spin $S = 3/2$ the zero-frequency peak at

FIG. 2 (color online). Dependence of T_K on the transverse
anisotropy B_2/D: (a) T_K from the full NRG calculation,
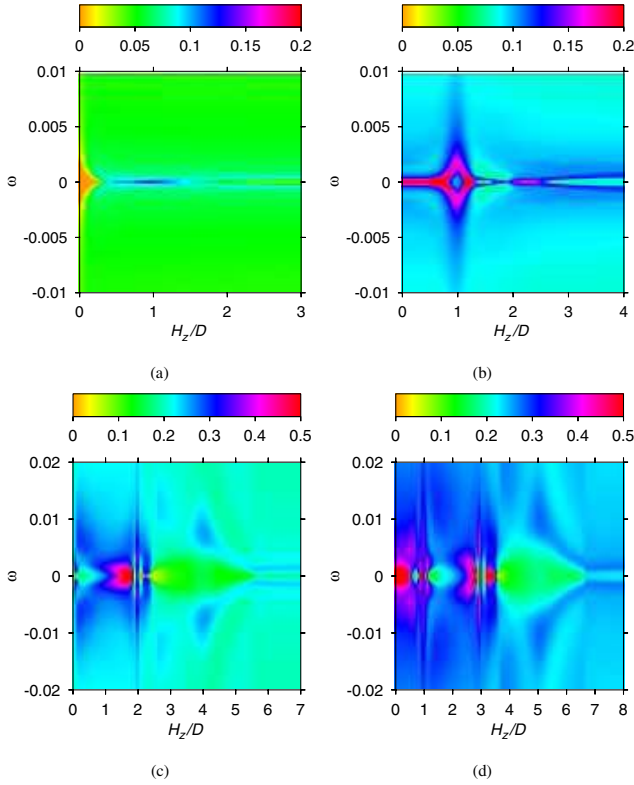(b) spin-binding energy estimate ΔE. Parameters: $S = 7/2$, $D =
10^{-4}$ W.

FIG. 3 (color online).   Spectral function, qualitatively equivalent to dI/dV_{bias} as function of H_z/D and frequency ω (a) for smallest nontrivial integer spin $S = 1$, (b) half-integer spin $S = 3/2$, and (c) large integer $S = 3$, (d) half-integer spin $S = 7/2$. Parameters: $J = 0.15$ W, $D = 10^{-4}$ W, and $B_2/D = 0.1$.

$H_z = 0$ in Fig. 3(b) is broadened with increasing H_z. This broadening is maximal at $H_z = D$ and is also captured by the H_z/D dependence of the spin-binding energy ΔE (not shown). The full NRG result in addition shows a sharp dip superimposed on the broad peak at $H_z = D$ (anticrossing of $|1+\rangle$ and $|2+\rangle$). At this point the situation is very similar to the $S = 1$ case, provided one neglects the contribution of the low lying state $|2-\rangle$ and reduces the magnetic field by D, see Fig. 1. Indeed, increasing the field further to $H_z = 2D$, the Kondo effect reappears precisely as for $S = 1$ near $H_z = D$. For larger spin the physics is qualitatively the same: the spectral function in Figs. 3(c) and 3(d) displays *several* dips of the Kondo peak close to each anticrossing. The correspondence pointed out above is more general: the linear conductance of a SMM with spin S at magnetic field H_z corresponds qualitatively to that of a SMM with reduced spin $S - 1/2$ and reduced magnetic field $H_z - D$. This can be shown using the Hamiltonian Eq. (4) in the molecular eigenbasis. For fixed J the correspondence in the conductance is most obvious for subsequent S values. The conductance for spin S near $H_z = nD$ ($n = 1, 2, \ldots, 2S - 1$) can even be compared with that for $S - n/2$ around *zero field* by iterating n times, which we have checked. However, a clear correspondence appears only when J is properly adjusted.

Conclusion.—Magnetic field Kondo-transport spectroscopy can determine the absolute value of the spin and the magnetic parameters of a SMM in a transport junction. The strong Kondo effect in SMMs discussed in this work can be accessed experimentally by increasing the exchange coupling. In STM setups one can reduce the distance to the molecule, or change the molecular geometry by a bias-voltage pulse [19]. In 3-terminal measurements [2,3] one can tune the exchange coupling with the gate voltage: $J \propto 1/|V_g^* - V_g|$. In addition, both the charge and spin state can be changed by tuning the gate voltage to opposite sides of the charge degeneracy point $V_g = V_g^*$. If a single-electron transport current [6] is observed at this point, cf. [2,3], S only changes by $1/2$. Then the predicted clear correspondence between the linear conductance for subsequent integer and half-integer spin values provides an additional check on the physics. Importantly, the spectroscopy can be done at temperatures above the energy scale of the magnetic splittings and requires only low magnetic fields which do not destroy the Kondo effect by Zeeman splittings. Finally, we have checked that a small fixed transverse magnetic field perturbation does not destroy the reentrant behavior of the Kondo effect as the longitudinal field is varied.

[1] D. Gatteschi and R. Sessoli, Angew. Chem., Int. Ed. **42**, 268 (2003), and references therein.
[2] H. Heersche *et al.*, Phys. Rev. Lett. **96**, 206801 (2006).
[3] M.-H. Jo *et al.*, Nano Lett. **6**, 2014 (2006).
[4] G.-H. Kim and T.-S. Kim, Phys. Rev. Lett. **92**, 137203 (2004).
[5] C. Romeike, M. R. Wegewijs, W. Hofstetter, and H. Schoeller, Phys. Rev. Lett. **96**, 196601 (2006).
[6] C. Romeike, M. R. Wegewijs, and H. Schoeller, Phys. Rev. Lett. **96**, 196805 (2006).
[7] D. Goldhaber-Gordon *et al.*, Nature (London) **391**, 156 (1998).
[8] S. M. Cronenwett, T. H. Oosterkamp, and L. P. Kouwenhoven, Science **281**, 540 (1998).
[9] F. Simmel *et al.*, Phys. Rev. Lett. **83**, 804 (1999).
[10] J. Schmid, J. Weis, K. Eberl, and K. v. Klitzing, Phys. Rev. Lett. **84**, 5824 (2000).
[11] W. G. van der Wiel *et al.*, Science **289**, 2105 (2000).
[12] J. Park *et al.*, Nature (London) **417**, 722 (2002).
[13] W. Liang *et al.*, Nature (London) **417**, 725 (2002).
[14] L. I. Glazman and M. E. Raikh, JETP Lett. **47**, 452 (1988).
[15] T. K. Ng and P. A. Lee, Phys. Rev. Lett. **61**, 1768 (1988).
[16] K. G. Wilson, Rev. Mod. Phys. **47**, 773 (1975).
[17] W. Hofstetter, Phys. Rev. Lett. **85**, 1508 (2000).
[18] T. A. Costi, Phys. Rev. Lett. **85**, 1504 (2000).
[19] V. Iancu, A. Deshpande, and S.-W. Hla, Nano Lett. **6**, 820 (2006).